Open Access

Surface Plasmon Resonance Based Titanium Coated Biosensor for Cancer Cell Detection

Md. Asaduzzaman Jabin, *Member, IEEE*
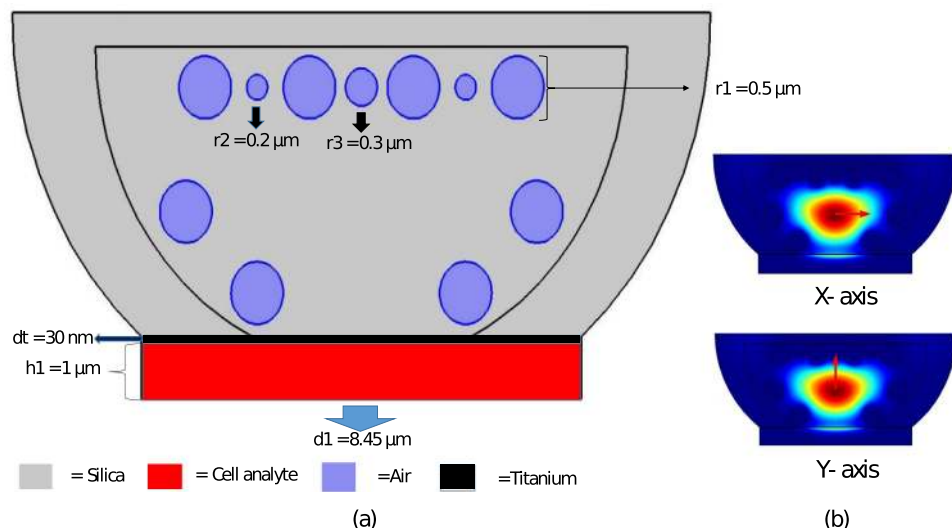Kawsar Ahmed, *Member, IEEE*
Md. Juwel Rana, *Member, IEEE*
Bikash Kumar Paul, *Member, IEEE*
Maheen Islam, *Member, IEEE*
Dhasarathan Vigneswaran, *Member, IEEE*
Muhammad Shahin Uddin

Surface Plasmon Resonance Based Titanium Coated Biosensor for Cancer Cell Detection

Md. Asaduzzaman Jabin [1] *Member, IEEE,*
Kawsar Ahmed [1,2] *Member, IEEE,* **Md. Juwel Rana,**[1] *Member, IEEE,*
Bikash Kumar Paul [1,2,3] *Member, IEEE,*
Maheen Islam [4] *Member, IEEE,*
Dhasarathan Vigneswaran [5] *Member, IEEE,*
and Muhammad Shahin Uddin[1]

[1]Department of Information and Communication Technology, Mawlana Bhashani Science and Technology University, Tangail 1902, Bangladesh
[2]Group of Biophotomatiχ, Mawlana Bhashani Science and Technology University, Tangail 1902, Bangladesh
[3]Department of Software Engineering, Daffodil International University, Dhaka 1207, Bangladesh
[4]Department of Computer Science and Engineering, East West University, Dhaka 1212, Bangladesh
[5]Department of Physics, University College of Engineering Ramanathapuram, Ramanathapuram 623 513, India

Abstract: A new optimized bowl-shaped mono-core surface plasmon resonance based cancer sensor is proposed for the rapid detection of different types of cancer affected cell. By considering the refractive index of each individual cancer contaminated cell with respect to their normal cell, some major optical parameters variation are observed. Moreover, the cancerous cell concentration is considered at 80% in liquid form and the detection method is finite element method with 2 100 390 mesh elements. The variation of spectrum shift is obtained by plasmonic band gap between the silica and cancer cell part which is separated by a thin (35 nm) titanium film coating. The proposed sensor depicts a high birefringence of 0.04 with a maximum coupling length of 66 μm. However, the proposed structure provides an optimum wavelength sensitivity level between about 10 000 nm/RIU and 17 500 with a resolution of the sensor between 1.5×10^{-2} and 9.33×10^{-3} RIU. Also, the transmittance variance of the cancerous cell ranges from almost 3300 to 6100 dB/RIU and the amplitude sensitivity ranges nearly between -340 and -420 RIU^{-1} for different cancer cells in major polarization mode with the maximum detection limit of 0.025. Besides, the overall sensitivity performance is measured with respect to their normal cells which can be better than any other prior structures that have already proposed.

Index Terms: Cancer cells, Cancer Sensing and Detection, Mono-core Bowl shaped SPR, Birefringence, and Sensitivity.

1. Introduction

The surface plasmon resonance (SPR) has already proved its strong potentiality in sensing application. Generally, SPR consists of a silica-core with small circular air bubbles through the length of the

fiber [1]. In order to get better flexibility in design, we have to consider finite element method (FEM) based a full vector software COMSOL Multiphysics version 5.1. But nowadays, SPR based photonic crystal fiber (PCF) can be used for the sensing, diagnosis and the detection of diseases to ensure the better treatment in biomedical science. Clark *et al.* introduced the first biosensor for glucose detection from blood [2]. Day by day, different methods like – micro-fluid [3], electro-chemical [4], immune-chemistry [5] and molecular- level cancer identification [6] have been introduced. After the development of different regions, Yaroslavsky *et al.* proposed a carcinoma cancer detection [7], the photonic-thermal effect on nano-composite structure [8] and cancer exists in the body fluid [9], [10]. Sun *et al.* demonstrated breast cancer (HER-2) bio-mark [11]. But, all the following models of the cancer cell detection were based only on Basal cell with the sensitivity level less than 7000 nm/RIU or gave sensitivity measurement with respect to the other cancerous cell parameters. But, our proposed model provides a promising performance with optimized sensing in the rapid detection of cancer from cell liquid (80% concentration) with respect to its normal cell (30–70% concentration). As we know that, the various cancer viruses evident with different optical parameters variation for their internal protein structure. Besides, the refractive index of normal cells and the cancerous cells will be different. This refractive index response helps to easily differentiate the normal and cancerous cells. So, the proposed model will be the better option than any other prior models that have ever built.

In this article, a SPR based optical sensor has been introduced for the rapid detection of different types of cancer affected cell such as- blood cancer (Jurkat), cervical cancer (HeLa), adrenal glands cancer (PC12), 2 types of breast cancer (MDA-MB-231 and MCF-7) and skin cancer (Basal) etc. Moreover, the cancerous cell concentration is considered at 80% in liquid form and the detection method is FEM. The proposed bowl-shaped SPR PCF based cancer detection sensor has been investigated for the wide spectrum ranging from 0.5 μm to 2.0 μm. The aim is to report a fabrication friendly sensor that can achieve high amplitude and wavelength sensitivity, low loss, and high birefringence. The proposed methodology will be opened a new dimension of cancer cell detecting.

2. Geometry and Anatomy of PCF

The bi-sectional view of the proposed model mainly is consisted with a bowl-shaped structure with mono-core transmission modes. It contains fused silica as a background and PML material. The internal lattice arrangement is bounded in the core region that contains a ring structure using a series of air holes where, hole diameters, r1 = 0.5 μm, r2 = 0.2 μm, r3 = 0.3 μm and pitch p = 2 μm to vary the mode confinement that is described in Fig. 1(a). A single layer of bio-sample is set up at the bottom of the structure which is separated from the silica with a thin titanium coating d_t = 30 μm. The variations of big air holes affect the sensitivity of the bio-samples. The refractive indices and dielectric constants of the bio-samples are displayed in Table 1. But, the sensitivity variation of each cancerous cell can be evaluated with respect to their individual unaffected cells. Besides, the proposed model is a more optimized and extended version of D-shaped PCF which gives more flexibility in optical parameters and increases the sensing performance. In D-shape SPR PCF, the analyte layer is attached at the flat part of "D". But, in our model it is attached at the bottom of "D" which gives more stability and robustness in sensing. Because, the distance between center of fiber core and metal layer provides space to well form of the full radius of core that results the increment of plasmon. However, in case of conventional D-shape, the core is not getting well-formed at the analyte side that causes the reduction of plasmon. As a result, sensitivity response will be less. Due to the simple design, the proposed sensor can be fabricated by current technology like- sol-gel, extrusion and drilling technique. Imperfect fabrication of air holes does not affect so much because a PCF biosensor relies on surface plasmon incident which occurs on metal-anlyte boundary. However, air holes are used as a fence of core mode that is not related to plasmonic incident. So, it should be only applicable for just PCF but not for SPR based PCF.

With the best of knowledge, this type of D-PCF structure is introduced for the first time as an optical sensor. In addition, for the very first time, different cancer cells are also sensed by employing titanium coated refractive index based biosensor for wider spectrum.
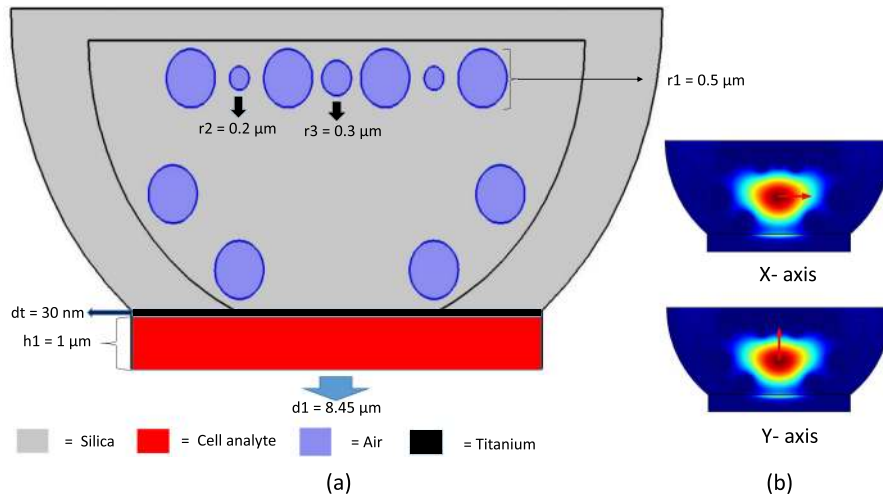
Fig. 1. (a) The schematic diagram of bowl-shaped SPR PCF cancer sensor with geometrical parameters like- the diameter of hole r1 = 0.5 μm, r2 = 0.2 μm, r3 = 0.3 μm and pitch constant p = 2 μm. (b)The direction of electrical field distribution in X and Y-polarization mode.

TABLE 1

The Refractive Indices for Jurkat, HeLa, PC12, MBA-MD-231, MCF-7 and Basal Cancerous Cell As Well As Their Corresponding Normal Cells

Cell Name	Cell type and Concentration Level	Refractive Index	Reference
Jurkat	Blood Cancer (80%)	1.39	[13] − [20]
	Normal cell (30–70%)	1.376	[13] − [20]
HeLa	Cervical Cancer (80%)	1.392	[13] − [17]
	Normal cell (30–70%)	1.368	[13] − [17]
PC12	Adrenal Glands Cancer (80%)	1.395	[13] − [20]
	Normal cell (30–70%)	1.381	[13] − [20]
MDA-MB-231	Breast Cancer (80%)	1.399	[13] − [17]
	Normal cell (30–70%)	1.385	[13] − [17]
MCF-7	Breast Cancer (80%)	1.401	[13] − [20]
	Normal cell (30–70%)	1.387	[13] − [20]
Basal	Skin Cancer (80%)	1.38	[12],[13],[20]
	Normal cell (30–70%)	1.36	[12], [13], [20]

3. Theoretical Analysis

The main goal of the proposed cancer sensor is to detect cancer by FEM method and create plasmonic resonance to define the total variation of the absorption of light by the desired bio-sample. In order to calculate the outcome of the coupling length of the mono-core structure, the transmission- spectrum, wavelength sensitivity (nm/RIU) and transmittance variance (dB/RIU) are evaluated from the effects in different modes of X and Y-polarization of bowl-shaped SPR. In order to classify these modes into two groups: (1) X-polarization modes (n^x) and (2) Y-polarization modes

(n^y) for the proposed SPR PCF, the deep mode confine is mandatory and their polarization is shown in Fig. 1(b). The effective RI of the proposed model is derived from Sellmeier's RI equation for fused silica material [20] can be defined by,

$$n \text{ (RIU)} = sqrt\left(1 + \frac{B_1\lambda^2}{\lambda^2 - C_1} + \frac{B_2\lambda^2}{\lambda^2 - C_2} + \frac{B_3\lambda^2}{\lambda^2 - C_3}\right) \tag{1}$$

Where, n is the effective RI of the fused-silica material and $B_1 = 0.696163$, $B_2 = 0.4079426$, $B_3 = 0.8974794$, $C_1 = 0.0046914826 \ \mu m^2$, $C_2 = 0.0135120631 \ \mu m^2$ and $C_3 = 97.9340025 \ \mu m^2$ are Sellmeier's constants respectively for fused silica material. The birefringence or RI difference between different super modes of X and Y polarization of the Bowl-Shaped SPR [19], [20] can be evaluated by,

$$B = \Delta n_{xy} = \left|n_x^i - n_y^i\right| \tag{2}$$

Here, i = X or Y-polarization of the proposed model. Using Eq. (2), the entire variation of RI difference between different modes is considered with respect to the wavelength for X and Y polarization. For any plasmonic structure, it faces a problem with mode confinement loss that cannot be removed from the structure. Generally, confinement-loss is used to define the sensitivity of the structure. The confinement-loss of the proposed model can be calculated by,

$$\alpha_c \text{ (dB/cm)} = 8.686 \times \frac{2\pi}{\lambda} \times 10^4 \tag{3}$$

Here, λ = wavelength that is considered for the proposed structure. Generally, coupling-length defines as the minimum length at which the maximum amount of light that can easily be passed through the small silica core. The coupling-length of the mono core L_c in X and Y polarization for the bowl-shaped SPR PCF [19], [20] can be evaluated by,

$$L_c \text{ } (\mu m) = \frac{\lambda}{2|n_x^i - n_y^i|} \tag{4}$$

From the Eq. (4), we have to calculate the coupling-length of the bowl-shaped SPR PCF cancer sensor for different wavelength. It is evident that the coupling-length is inversely proportional to the wavelength. An optical field passes through the mono core that enables by the proposed structure which also supports to acquire a better cancer sensing. In order to calculate the sensing, the output of the optical power which passes through the silica core [20] is defined by,

$$P_{out} \text{ } (watt) = \sin^2\left(\frac{|n_x - n_y|\pi L}{\lambda}\right) = \sin^2\left(\frac{\Delta n_{xy}\pi L}{\lambda}\right) \tag{5}$$

Here, L indicates the total length of the fiber. Hence, we can evaluate the optical power passes through the mono-core along the proposed PCF with a variable fiber length L, according to Eq. (5). When the light passes through the proposed fiber, the transmittance spectrum [19], [20] can be evaluated by,

$$T_r \text{ (dB)} = 10 \times log_{10}\left(\frac{P_{out}}{P_{in}}\right) \tag{6}$$

Here, P_{in} and P_{out} are defined as the maximum input and output power. However, the wavelength sensitivity of the proposed sensor can be calculated through the shift of sharp zenith of the transmittance curve on a specific wavelength for the total variation of RI. The wavelength sensitivity with respect to density level [18], [19] and [20] can be defined as,

$$S_w \text{ (nm/RIU)} = \frac{\Delta\lambda_p}{\Delta n} \tag{7}$$

Here, $\Delta\lambda_p$ defines as the variation of peak wavelength and Δn defines the variation of RI of cancer cells. Thus, the sensitivity of a cancer cell is evaluated from Eq. (7) and transmittance curve can be

varied with the transmittance variance or T_r sensitivity,

$$S_v \text{ (dB/RIU)} = \frac{\max(tx_{b1} - tx_{b2})}{\max(n_{b1} - n_{b2})} \tag{8}$$

Here, $\triangle n_b$ is the RI difference between two bio-samples (normal and cancerous) and tx_{b_1, b_2} are the T_r curve of maximum amplitude for b_1, b_2 bio-samples, respectively. But, any change in RI of the bio-samples can be easily detected by the variation of the resolution of the proposed structure. So, the resolution of the proposed model can be evaluated by,

$$RI \text{ (RIU)} = \frac{\triangle n \times \triangle \lambda_{\min}}{\triangle \lambda_{peak}} \tag{9}$$

Here, $\triangle n$ is the difference of RI, $\triangle \lambda_{\min}$ and $\triangle \lambda_{peak}$ are respectively for the minimum and peak wavelength difference, respectively, for that specific RI of the normal cell and cancerous cell for the corresponding cancer detection. So, the values of $\triangle$ n are 0.014, 0.024, 0.014, 0.014, 0.014, and 0.02, $\triangle \lambda_{\min}$ is 0.1 nm and $\triangle \lambda_{peak}$ are 0.2, 0.17, 0.14, 0.15, 0.16, and 0.13 nm for the corresponding cancer cells. The resolution of the sensor directly affects the phase detection method to control the amplitude interrogation method. The complexity of the amplitude interrogation method can be removed by using the amplitude sensitivity equation. The amplitude sensitivity of the proposed cancer sensor can be evaluated by,

$$S_a \text{ (RIU}^{-1}) = -\frac{1}{\alpha_c} \times \frac{\triangle \alpha_c}{\triangle n} \tag{10}$$

Here, α_c is the confinement-loss of the particular bio-samples, α_c and $\triangle n$ define as the loss difference and RI difference between normal and cancerous cells, respectively.

4. Result Analysis and Discussion

All the figures in this paper depict the optical parameters for the normal and the cancer affected cell bio-samples as a function of wavelength. The dotted line represents the normal cell and the continuous line represents the cancerous cell. Besides, the triangular marker shows the curve for X-axis and circular marker demonstrates the curve for the Y-axis. Fig. 2 demonstrates the response of RI with respect to the variation of wavelength. It can clearly be noticed that the RI of the bio-samples is smoothly in downward sloping. The RI interrogative curve displays a linear structure with a straight line. The RI of any bio-samples starts from its maximum value and gradually decreasing its value to the minimum value. If we change the RI for different bio-samples it will affect the entire system in a linear manner. The maximum possible RI of the bio-samples ranges remain between about 1.445 and 1.47. Last of all, the RI of the normal cell (30–70%) and the cancerous cell (80%) are looking forward to getting so close to each other. This behavior will throw an open challenge to effective cancer sensing mechanism.

Figs. 3 and 4 depict the confinement-loss spectrum for X and Y-polarization vs. wavelength along with the spp polarization mode and core polarization mode. It is evident that the intersecting point of the core guiding mode and spp guiding mode gives the highest peak value of the maximum confinement loss for each individual cancer cell bio-samples. Here, the proposed model gives few intersecting points at wavelength 1.25 μm, 1.41 μm, 1.57 μm, 1.72 μm, 1.88 μm, 1.92 μm and 1.27 μm, 1.42 μm, 1.59 μm, 1.73 μm, 1.87 μm, 1.93 μm respectively for X and Y-polarization of the corresponding cancer cell bio-samples. It also defines that the proposed sensor gives maximum sensitivity at that particular point. The corresponding confinement loss curves show almost 930 dB/cm, 1020 dB/cm, 1060 dB/cm, 1100 dB/cm, 1160 dB/cm and 1200 dB/cm for X-polarization and 700 dB/cm, 810 dB/cm, 960 dB/cm, 1010 dB/cm, 1100 dB/cm and 1180 dB/cm for Y-polarization for the proposed cancer model. The loss curve and intersecting point of the core mode and spp-mode define the amplitude sensitivity and mode-resolution of the proposed cancer sensor.

Fig. 5 depicts the amplitude sensitivity with respect to the wavelength for different cancerous cell bio-samples. The proposed model provides a sharp negative peak of amplitude sensitivity for each
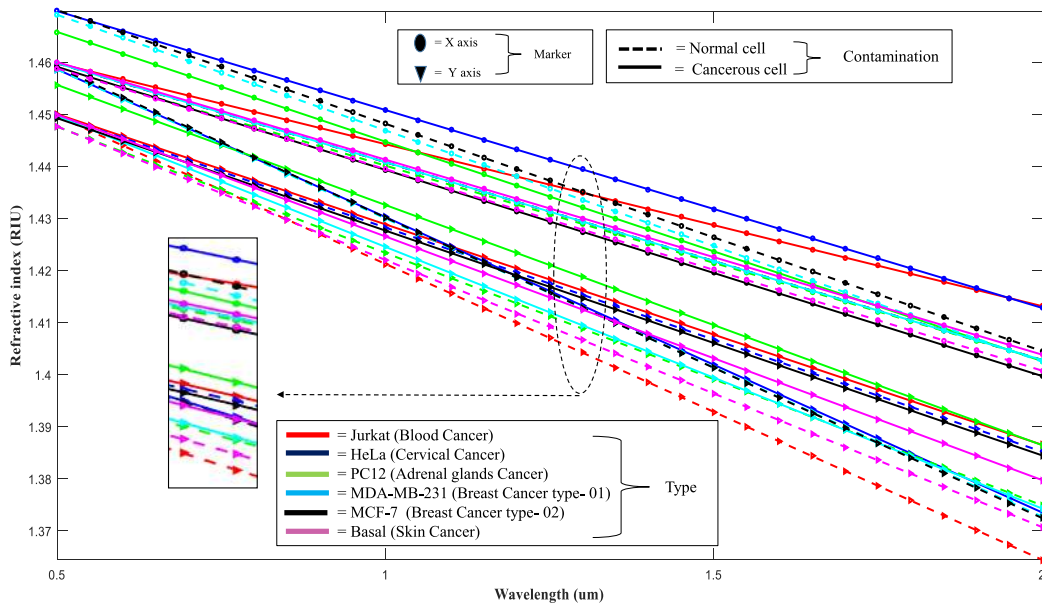
Fig. 2. The effective refractive index of X and Y–polarization vs. wavelength for different cancer cells at 80% concentration level for the proposed structure.
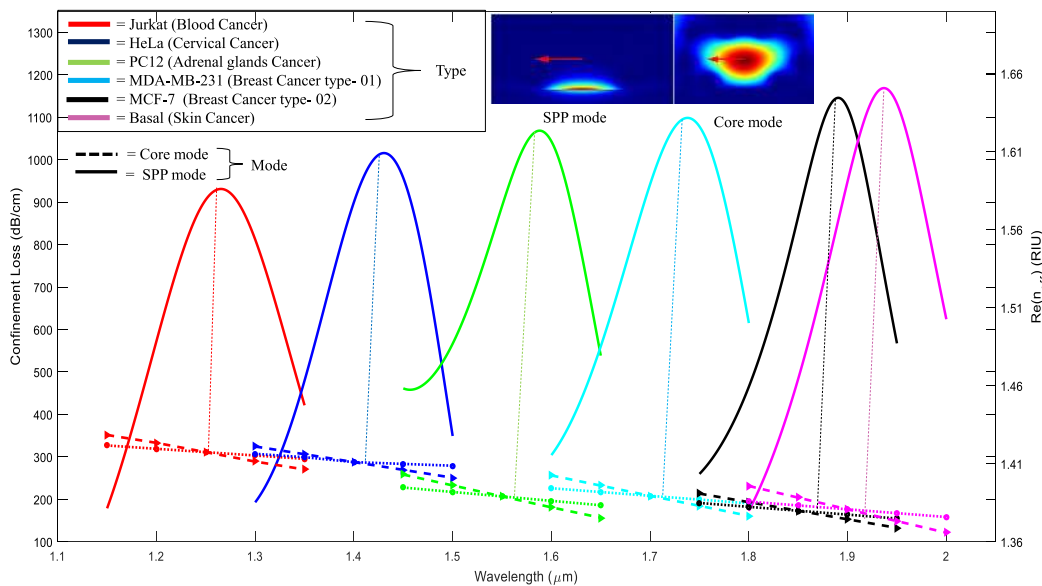

Fig. 3. The mode confinement loss of X–polarization vs. wavelength for different cancer cells along with SPP mode and core mode at 80% concentration level for the proposed structure.

individual cancerous cell bio-samples. The maximum amplitude sensitivity for each corresponding cancer cell bio-samples are almost -330 RIU^{-1}, -340 RIU^{-1}, -375 RIU^{-1}, -380 RIU^{-1}, -410 RIU^{-1} and -430 RIU^{-1} that are briefly described in Table 2. It is evident that the proposed model depicts more sensitive to the amplitude variation of the corresponding cancer cell bio-samples which enhances the resolution of the proposed cancer sensor. The maximum interrogative resolution the proposed cancer sensor are almost 7×10^{-3}, 1.4×10^{-2} RIU, 1.0×10^{-2} RIU, 9.33×10^{-3} RIU, 8.75×10^{-3} RIU, 1.5×10^{-2} RIU. In this case, the proposed cancer sensor can proof itself better than any other prior models. Sensing of bio-samples on SPR based PCF greatly depends on
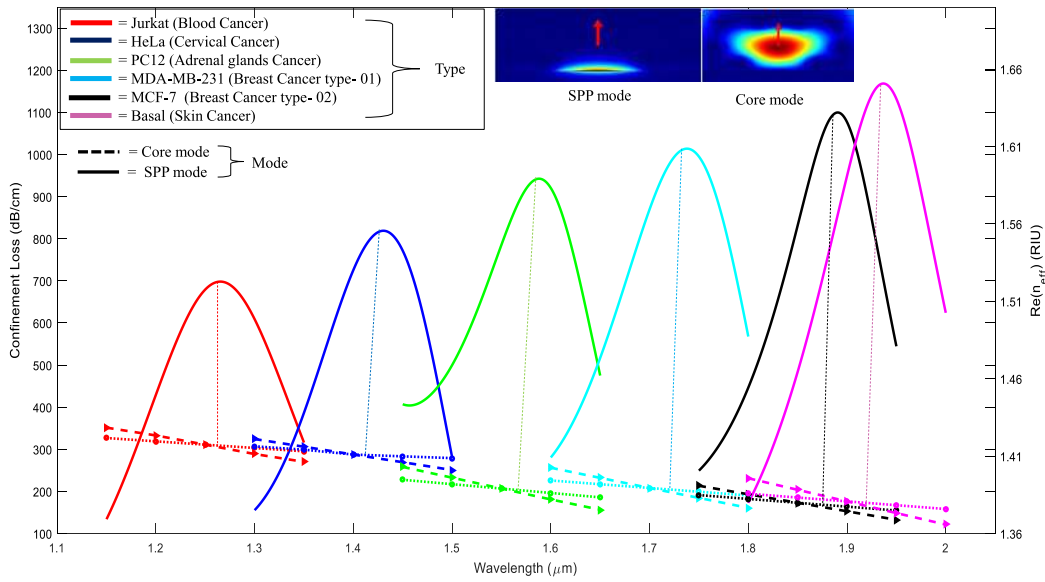
Fig. 4. The mode confinement loss of Y–polarization vs. wavelength for different cancer cells along with SPP mode and Core mode at 80% concentration level for the proposed structure.
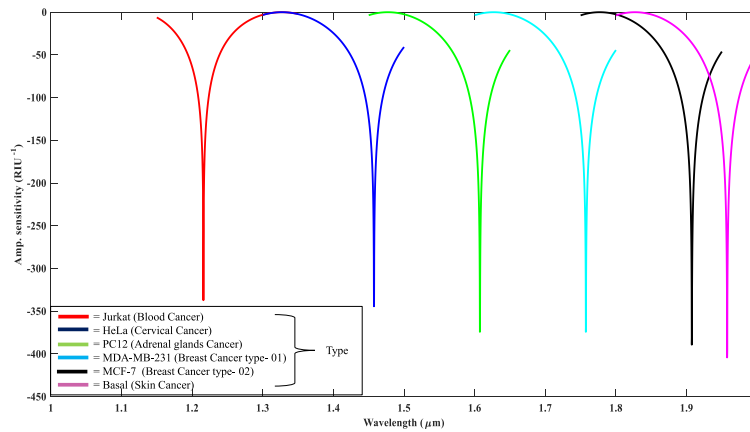

Fig. 5. The amplitude sensitivity vs. wavelength for the proposed structure.

TABLE 2
The Relative Sensitivity Profiles for Jurkat, HeLa, PC12, MBA-MD-231, MCF-7, Basal Cancerous Cell
in Terms of Their Normal Cells

| Cell Name	Cell and Density Level	$S_w(nm/RIU)$	$S_a(RIU^{-1})$	$Rl(RIU)$	$S_v(dB/RIU)$	Detection Limit
Jurkat	Blood Cancer (80%)	10714.28	-330	7×10^{-3}	5357.14	0.014
HeLa	Cervical Cancer (80%)	10208.33	-340	1.4×10^{-2}	3333.33	0.024
PC12	Adrenal Glands Cancer (80%)	10000	-375	1.0×10^{-2}	5357.14	0.014
MDA-MB-231	Breast Cancer (80%)	17857.14	-380	9.33×10^{-3}	6071.42	0.014
MCF-7	Breast Cancer (80%)	18071.42	-410	8.75×10^{-3}	5642.85	0.014
Basal	Skin Cancer (80%)	17500	-430	1.5×10^{-2}	3900	0.02
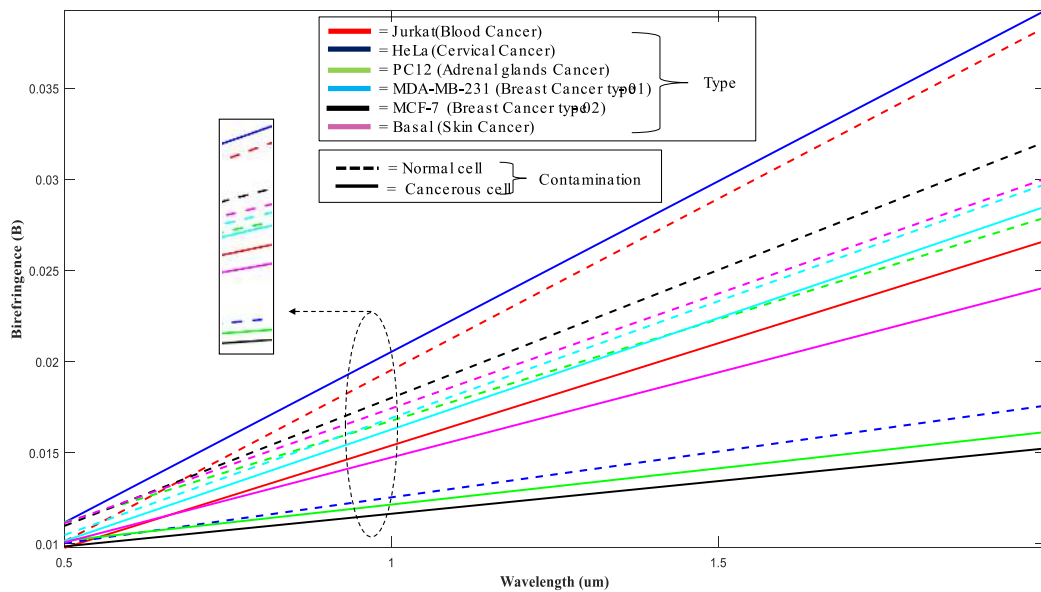
Fig. 6. The birefringence response vs. wavelength for the proposed structure.

the birefringence of the plasmon. Fig. 6 shows the total variation of birefringence with respect to wavelength variation for the normal cell (30–70%) and cancerous cell (80%).

It can clearly be said that the maximum possible birefringence ranges from almost 0.015 to 0.04 which shows an upward trending curve and the birefringence of the proposed structure directly affects its coupling length and wavelength sensitivity. It can be easily said that the birefringence of the corresponding cancer cells maintains a linear manner on a straight line with respect to the variation of the assumed wavelength. The birefringence of the proposed sensor starts from 0.015 and gradually increases in linear manner with the variation of the wavelength to an endpoint of high birefringence of 0.04.

Fig. 7 represents a smooth changing of coupling length with the variation of wavelength for the normal cell (30–70%) and the cancerous cell (80%). From the figure, it can clearly be evident that the maximum possible coupling length ranges between almost 25 μm and 66 μm which depicts an upward curly trending manner. Moreover, the transmittance is directly affected by the coupling length of the proposed model. The transmittance of the proposed model demonstrates the sensing performance of the cancer sensor. Fig. 8 shows the variation of transmittance with respect to the changing of the wavelength for the normal cell (30–70%) and the cancerous cell (80%). From the figure, it can be easily clarified that the maximum possible transmittance ranges almost between −100 dB to −200 dB and the needlepoint for each and every cell bio–sample show the highest sensing performance at that particular point. Using Eq. (6), (7) and (8) at Table 2, the optimum wavelength sensitivity level is observed almost for blood cancer is 10714.28 nm/RIU, cervical cancer is 10208.33 nm/RIU, adrenal glands cancer is 10000 nm/RIU, breast cancer (MDA-MB-231 cell is 17857.14 nm/RIU and MCF-7 cell is 18071.42 nm/RIU) and skin cancer is 17500 nm/RIU for different polarization mode with the maximum detection limit of 0.025. The transmittance-variance or sensing for blood cancer (Jurkat cell) sensitivity is almost 5357.14 dB/RIU, cervical cancer (HeLa cell) sensitivity is about 3333.33 dB/RIU, adrenal glands cancer (PC12 cell) sensitivity is nearly 5357.14 dB/RIU, breast cancer (MDA-MB-231) sensitivity is approximately 6071.42 dB/RIU, breast cancer (MCF-7) sensitivity is about 5642.85 dB/RIU and skin cancer (Basal) sensitivity is almost 3900 dB/RIU.

The main disadvantage of the prior models was the sensing of one cancer cell that depends on the neighboring cancer cell's performance. They only evaluated one cancerous cell with respect to another cancerous cell. Hence, the main goal of the proposed structure is to detect various types
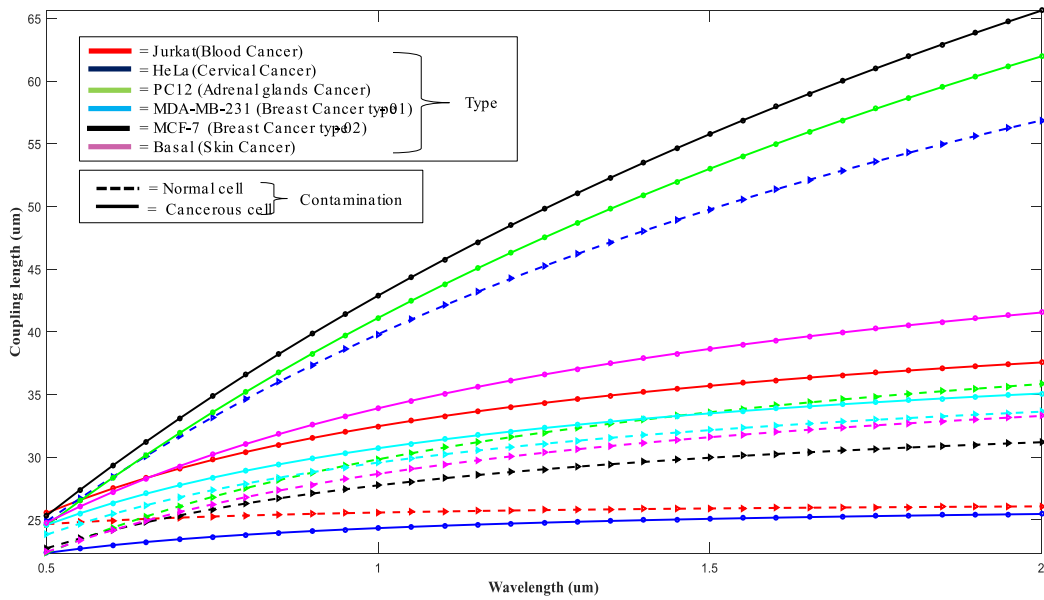
Fig. 7. The coupling length vs. wavelength for different cell bio-samples in X and Y–polarization of the proposed bowl-shaped PCF.
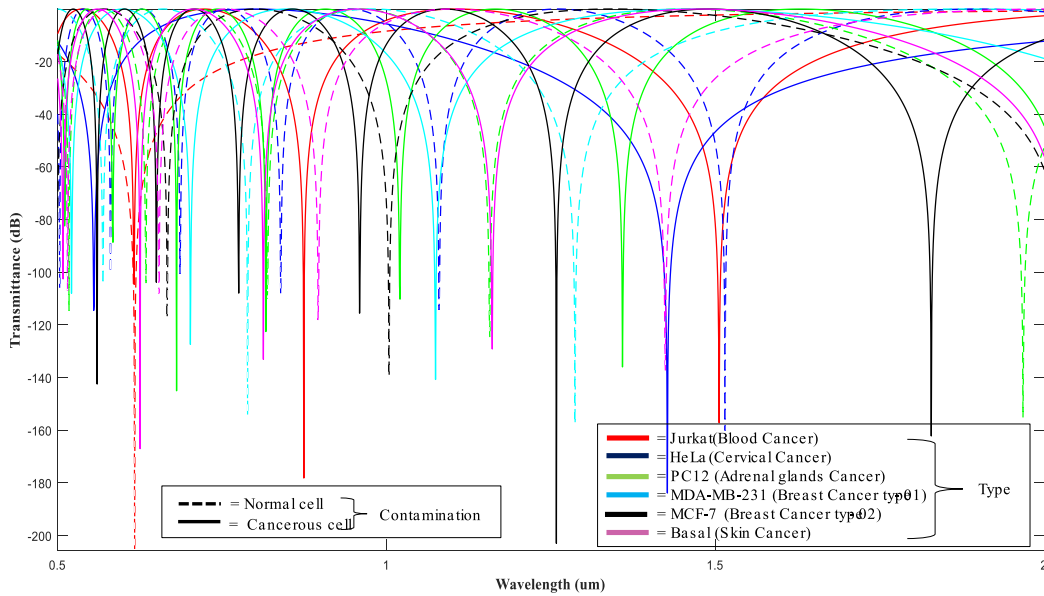

Fig. 8. The calculated transmittance of the proposed structure as a function of wavelength for different cell bio-samples of X and Y–polarization.

of cancer cell bio-samples with respect to their normal cell. This is the most effective way of cancer sensing.

5. Conclusion

The proposed model is the more optimized and extended version of D-shape PCF which provides more flexibility in the optical parameters and increase in sensing performance. Last but not the least, the proposed model can prove itself better than any other existing and prior models with these

effective optical parameters and wavelength sensing performance is almost 10714.28 nm/RIU, 10208.33 nm/RIU, 10000 nm/RIU, 17857.14 nm/RIU, 18071.42 nm/RIU and 17500 nm/RIU for different polarization mode, transmittance variance is about 5357.14 dB/RIU, 3333.33 dB/RIU, 5357.14 dB/RIU, 6071.42 dB/RIU, 5642.85 dB/RIU and 3900 dB/RIU and amplitude sensitivity is nearly about -330 RIU^{-1}, -340 RIU^{-1}, -375 RIU^{-1}, -380 RIU^{-1}, -410 RIU^{-1} and -430 RIU^{-1} with resolution level from 9.33×10^{-3} RIU to 1.5×10^{-2} RIU respectively for blood, cervical, adrenal, breast [type-1, 2] and skin cancer respectively with a maximum detection limit which is almost 0.025.

Acknowledgment

References

[1] E. K. Akowuah, H. Ademgil, S. Haxha, and F. A. Malek, "An endlessly single–mode photonic crystal fiber with low chromatic dispersion, and bend and rotational insensitivity," *J. Lightw. Technol.*, vol. 27, no. 17, pp. 3940–3947, Sep. 2009.
[2] L. Clark and Jr. Among, "Implantable gas– containing biosensor and method for measuring an analyte such as glucose," U.S. Patent 4 680 268, Jul. 14, 1987.
[3] L. Hajba and A. Guttman, "Circulating tumor-cell detection and capture using microfluidic devices," *TrAC Trends Anal. Chem.*, vol. 59, pp. 9–16, Jul./Aug. 2014.
[4] T. Li, Q. Fan, T. Liu, X. Zhu, J. Zhao, and G. Li, "Detection of breast cancer cells specially and accurately by an electrochemical method," *Biosensors Bioelectron*, vol. 25, no. 12, pp. 2686–2689, Aug. 2010.
[5] F.-R. Li, Q. Li, H.-X. Zhou, H. Qi, and C.-Y. Deng, "Detection of circulating tumor cells in breast cancer with a refined immunomagnetic nanoparticle enriched assay and nested-RT-PCR," *Nanomed. Nanotechnol. Biol. Med.*, vol. 9, no. 7, pp. 1106–1113, Oct. 2013.
[6] T. D. Bradley *et al.*, "Optical properties of low loss (70 dB/km) hypocycloid-core kagome hollow core photonic crystal fiber for Rb and Cs based optical applications," *J. Lightw. Technol.*, vol. 31, no. 16, pp. 2752–2755, Aug. 2013.
[7] J. Villatoro, V. Finazzi, V. P. Minkovich, V. Pruneri, and G. Badene, "Temperature-insensitive photonic crystal fiber interferometer for absolute strain sensing," *Appl. Phys. Lett.*, vol. 91, no. 9, p. 091109, Aug. 2007.
[8] A. N. Yaroslavsky *et al.*, "High-contrast mapping of basal cell carcinomas," *Opt. Lett.*, vol. 37, no. 4, pp. 644–646, 2012.
[9] J. Zhou, Y. Zheng, J. Liu, X. Bing, J. Hua, and H. Zhang, "A paperbased detection method of cancer cells using the photo-thermal effect of nanocomposite," *J. Pharmaceutical Biomed. Anal.*, vol. 117, pp. 333–337, Jan. 2016.
[10] N. Nallusamy, R. V. J. Raja, and G. J. Raj, "Highly sensitive nonlinear temperature sensor based on modulational instability technique in liquid infiltrated photonic crystal fiber," *IEEE Sensors J.*, vol. 17, no. 12, pp. 3720–3727, Jun. 2017.
[11] Y. Zhao, D. Wu, and R.-Q. Lv, "Magnetic field sensor based on photonic crystal fiber taper coated with ferrofluid," *IEEE Photon. Technol. Lett.*, vol. 27, no. 1, pp. 26–29, Jan. 2015.
[12] A. N. Yaroslavsky *et al.*, "High-contrast mapping of basal cell carcinomas," *Opt. Lett.*, vol. 37, no. 4, pp. 644–646, 2012.
[13] C. Tsai and S. Huang, Water Distribution in Cancer and Normal Cells. (2012). [Online]. Available: http://laser.ee.ntu.edu.tw/
[14] X. J. Liang, A. Q. Liu, X. M. Zhang, P. H. Yap, T. C. Ayi, and H. S. Yoon, "Determination of refractive index for single living cell using integrated biochip," in *Proc. IEEE 13th Int. Conf. Solid-State Sens., Actuators Microsyst.*, vol. 2, Jun. 2005, pp. 1712–1715.
[15] P. Sharma, P. Sharan, and P. Deshmukh, "A photonic crystal sensor for analysis and detection of cancer cells," in *Proc. IEEE Int. Conf. Pervasive Comput.*, Jan. 2015, pp. 1–5.
[16] E. A. Thomson, "MIT Radar Research Used to Treat Breast Cancer Enters Phase II Trials," *MIT Tech Talk.* (2001). [Online]. Available: http://news.mit.edu/2001/fenn-0110
[17] N. R. R. Anujam *et al.*, "Enhanced sensitivity of cancer cell using one dimensional nano composite material coated photonic crystal," *Microsystem Technol.*, vol. 25, no. 1, pp. 189–196, 2019.
[18] K. Ahmed *et al.*, "Refractive index based blood components sensing in terahertz spectrum," *IEEE Sens. J.*, vol. 19, no. 9, pp. 3368–3375, May 2019.
[19] N. Ayyanar, G. T. Raja, M. Sharma, and D. Kumar, "Photonic crystal fiber–based refractive index sensor for early detection of cancer," *IEEE Sensors J.*, vol. 18, no. 17, pp. 7093–7099, Sep. 2018.
[20] P. Sharan, S. M. Bharadwaj, F. D. Gudagunti, and P. Deshmukh, "Design and modelling of photonic sensor for cancer cell detection," in *Proc. IEEE Int. Conf. IMpact E-Technol. US*, Jan. 2014, pp. 20–24.